
BLIND CURVELET BASED DENOISING OF SEISMIC SURVEYS IN COHERENT AND INCOHERENT NOISE ENVIRONMENTS

A PREPRINT

Naveed Iqbal, Mohamed Deriche, Ghassan AlRegib, and Sikandar Khan

July 27, 2022

ABSTRACT

The localized nature of curvelet functions, together with their frequency and dip characteristics, makes the curvelet transform an excellent choice for processing seismic data. In this work, a denoising method is proposed based on a combination of the curvelet transform and a whitening filter along with procedure for noise variance estimation. The whitening filter is added to get the best performance of the curvelet transform under coherent and incoherent correlated noise cases, and furthermore, it simplifies the noise estimation method and makes it easy to use the standard threshold methodology without digging into the curvelet domain. The proposed method is tested on pseudo-synthetic data by adding noise to real noise-less data set of the Netherlands offshore F3 block and on the field data set from east Texas, USA, containing ground roll noise. Our experimental results show that the proposed algorithm can achieve the best results under all types of noises (incoherent or uncorrelated or random and coherent noise).

1 Introduction

Seismic surveys consist of large volumes of sensors. These sensors are laid on the earth surface to image the local geology for possible oil and gas reservoirs. Sound waves are produced using a source (vibrator). The waves bounce off various layers within the earth and reflected waves to the surface are captured by sensors. The recorded data is usually contaminated with unwanted energy or noise. One of the main challenges in processing seismic data is to remove/suppress noise in order to enhance the Signal-to-Noise Ratio (SNR) and later, avoid the false interpretation of seismic data [1–3], which can be detrimental. In general, seismic data processing can never eliminate noise completely, hence, the objective is to improve the SNR as much as possible. Successful removal of the noise results in an enhanced image of the subsurface geology, which facilitates economical decisions such as in hydrocarbon exploration. In [4], authors define the signal of interest as the signal energy that is coherent from trace to trace and desirable for

interpretation from geophysical prospective. Noise includes disturbances in seismic data caused by any unwanted seismic energy, such as multiples, shot generation ground roll, effects of weather (wind, rain), and human activities. Noise can also occur because of random occurrences within the earth. Broadly speaking, noise in seismic are classified as random noise, coherent noise and correlated noise [5, 6].

In short, noise in seismic surveys can be classified as follows:

- Incoherent noise: It is independent of the seismic source signal and there is no noise correlation among the traces.
- Correlated and uncorrelated noise: Incoherent noise can have correlation or no correlation among the noise samples within the trace and, hence, called as correlated (Browian noise [7], pink noise [8] and noise through geophone [9]) or uncorrelated (or random or additive white noise [10]) noise, respectively.
- Coherent noise: It is generated by the source and it is highly correlated with the source signal and across the traces. Figure 1 shows a case of coherent noise [11]. This noise is the most troublesome, since it can be highly correlated and aliased with the signal of interest [12].

Whatever are the causes or types of seismic noise, these result in significant artifacts that negatively impact the subsequent interpretation results, such as structural and spectral attributes, seismic imaging and analysis [13–16].

In this work, a novel and robust method is proposed based on the curvelet-transform using a data-whitening step which is able to deal with diverse and most challenging types of noise. The pre-whitening stage together with noise estimation from observation is collectively called as a blind curvelet based denoising method. The method is independent of type of noise and can be applied to variety of data sets. Therefore, the term “blind” is used to indicate that noise type is not needed to be known and method can be applied blindly. In summary, the main contributions of this work are as follows:

- The performance of the curvelet denoising is classified based on the types of images. For this purpose, seismic images and general purpose images are compared.
- A method to estimate noise from the seismic images for the coherent and incoherent noise cases is presented based on the pattern of the images. This simple and straightforward method is in contrast with previous methods in which curvelets need to be identified and nullified to remove the noise.
- It is shown that curvelet transform gives best performance for the white noise (uncorrelated). For the colored (correlated) noise, there is still room for improvement.
- Inherently, the curvelet transform works well for uncorrelated noise. For performance enhancement, pre-whitening and whitening inverse steps are introduced for the correlated noise case.
- Finally, the method which includes pre-whitening, noise estimation from the image and whitening inverse is adopted for the highly coherent case of ground roll noise.

- Synthetic, pseudo-synthetic and field data sets are used to demonstrate the effectiveness of the proposed curvelet transform based denoising method.

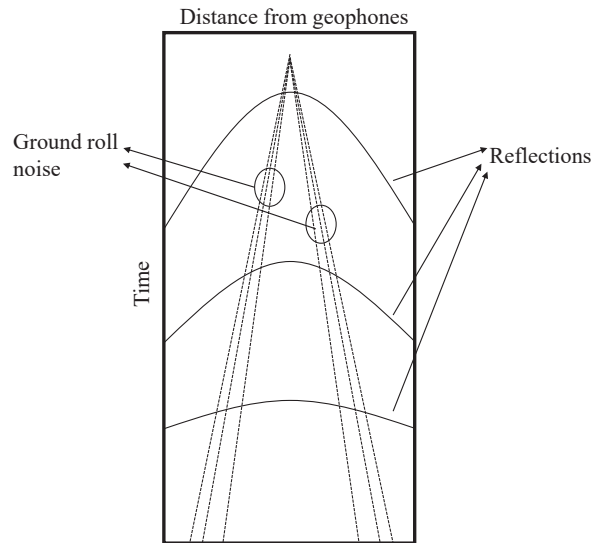


Figure 1: A pictorial view of ground roll noise and reflections.

2 Related Work

In this section, some of the noise removal/reduction techniques for seismic data are briefly discussed.

Band pass filtering and spectral filtering are common techniques used for enhancing the SNR in seismic applications. However, if signal and noise share the same frequency content then either one of these methods will result in signal attenuation and/or noise will not be fully removed. However, several other more complicated denoising methods have been proposed. The author in [17] discussed a particle-filter-based technique to enhance the SNR. When compared with other signal filtering methods, the particle filter offers an advantage of broad-band signal cleansing by directly modeling the internal dynamics of the target physical system and statistical characteristics of the signal and noise. In doing so, signal filtering can be related to the dynamic characteristics of the underlying physical system, rather than a purely mathematical operation. Deng *et al.* [18] discussed time-frequency peak filtering with an adaptive preprocessing to deal with the rapidly changing seismic wavelet. Furthermore, a threshold is designed to identify the noisy signal as a signal, buffer, or noise. In conventional time-frequency peak filtering, the Pseudo Wigner-Ville Distribution (PWVD) used for estimating the instantaneous frequency was shown to be sensitive to noise interferences that mask the borderline between the signal and noise, hence, detracting energy concentration. The authors in [19] presented a real-time Kalman filter, which removes the statistically described background noise from the recorded seismic traces. However, statistics of noise are not available in reality. Cai *et al.* [20] used the generalized S-transform to transform seismic data from the time-space to the time-frequency-space (t-f-x) domain. Then, the Empirical Mode

Decomposition (EMD) is applied on each frequency slice to suppress the coherent and random noise. An algorithm for wavelet denoising was proposed in [21] which used a wavelet-shrinkage estimate as a mean to design a wavelet-domain Wiener filter. The shrinkage estimate indirectly yields an estimate of the signal subspace that is leveraged into the design of the filter. The authors in [22] proposed an adaptive Singular-Value Decomposition (SVD) filter to enhance the non-horizontal events by the detection of seismic image texture direction and then horizontal alignment of the estimated dip through data rotation. The features derived from the co-occurrence matrix are used to estimate the texture direction. This technique works for random noise, however, some artifacts may appear.

Wiener filtering has been known for many decades and is considered to yield the optimum filter in the mean square sense. However, application of the Wiener filter directly for denoising problems in the seismic data requires statistical knowledge of the seismic source signal or noise which is not available in reality [23]. A different approach is to assume a particular type of noise, e.g. white Gaussian noise [6] or model noise as a linear/non-linear sweep signal for ground-roll noise elimination [5].

In this work, our aim is to develop a robust technique able to deal with diverse and most challenging types of noise, such as coherent noise (e.g. ground roll noise). It is worth mentioning that the denoising of ground roll noise is performed traditionally using band pass filtering [24]. This increases the SNR by attenuating the ground roll noise, however, the seismic data is also effected by this frequency filtering. The reason being that the band that is excluded by the filtering process may contain important seismic events. Consequently, the vertical resolution of the seismic data is lowered. To alleviate this, Oliveira *et al.* [25] proposed a curvelet based denoising method using hard thresholding. In this method, the authors identify the angular sections that contain the ground roll noise and erase the corresponding curvelet coefficients before reconstructing the seismic signal. The problem with this technique is that it requires visual inspection of the angular sections to identify the curvelet coefficients that are to be nullified to reduce noise. This process is demanding as it requires dedicated manpower to deal with the huge amount of data. A similar approach is also proposed in [26]. Recently, Górszczyk *et al.* [27, 28] proposed enhancement of 2-D and 3-D post-stack seismic data acquired in hardrock environment using 2-D curvelet transform. In their work, authors tackle random and colored noise. Scale-adjusted thresholding is introduced, which is a modification of [29], i.e., three levels are used for thresholding curvelet coefficients instead of two.

3 Curvelet Transform

The transform-domain denoising methods are the most effective techniques in seismic applications. These methods achieve the goal of noise removal or reduction by utilizing the properties of sparseness and separateness present in seismic data in the transform domain. Wavelet transforms are popular in scientific and engineering fields, however, they ignore the geometric properties of structures, regularity of edges and curvature nature of edges. The curvelet transform [30] is a multi-resolution directional transform which allows sparse representation of objects with curved edges. In comparison with the Fourier transform (sparse in frequency-domain and use translation only) and the wavelet

transform (sparse in time and frequency-domains and use translations and dilation), the curvelet transform is sparse in time, frequency and phase-domains, and uses translations, dilation and rotation.

In other words, the Fourier transform expresses a given time-domain signal, in terms of the amplitude and phase of each of the frequencies that are present in it. The wavelet transform is localized in both time and frequency whereas the standard Fourier transform is only localized in frequency. On the other hand, the curvelet transform is a higher dimensional generalization of the wavelet transform, which is designed to represent images at different scales and different angles. It basically overcomes the problem of missing directional selectivity of the wavelet transforms in 2-D signals (images). Another transform, known as the Gabor transform, also uses different directions and scales like curvelet. However, curvelets completely cover the whole spectrum, whereas, there are many holes (blank region) in the frequency plan of the Gabor filters [31].

There have been several other techniques of directional wavelet systems in recently proposed that have same goal, i.e., an optimal representation of directional features and a better analysis of signals in higher dimensions. These methods include steerable wavelets, Gabor wavelets, wedgelets, beamlets, bandlets, contourlets, shearlets, wave atoms, platelets, and surfacelets (these directional wavelets are uniformly called as X-lets). However, non of these methods has reached the same publicity as the curvelet transform. A good comparison of the above mentioned methods with curvelet can be found in [32]. In what follows, we will provide the mathematical background for the curvelet transform. The curvelet transform was initially developed by Candès and Donoho [33] and widely used for seismic data processing [27, 28, 34–36]. The curvelets are represented by a triple index, i.e., scale j , spatial location $k = (k_1, k_2)$, and orientation l . A curvelet at any scale j can be thought of an oriented object that has a support in the rectangle having width and length of 2^{-j} and $2^{-j/2}$, respectively, and obeys the parabolic scaling rotation width $\approx length^2$ [30]. The curvelet elements are obtained by parabolic translation, dilation and rotation of the specific function $\Phi_{j,l,k}$. The mother curvelet $\hat{\Phi}_j$ is defined in the frequency-domain as follows:

$$\hat{\Phi}_j(r, \omega) = 2^{-3/4} W(2^{-j}r) V\left(\frac{2^{\lfloor j/2 \rfloor} \omega}{2\Pi}\right), \quad (1)$$

where (r, ω) are the polar coordinates in the frequency-domain, $\lfloor j/2 \rfloor$ is the largest integer equal to or less than $j/2$, W is the radial window and V is the angular window. W and V are non-negative, smooth and real-valued functions and furthermore, these functions restrict the support $\hat{\Phi}_j$ to a polar wedge which is symmetric with respect to zero.

The curvelet $\Phi_{j,l,k}$ in the frequency-domain at scale 2^{-j} , orientation ψ_l and position $p_k^{j,l}$ is defined as:

$$\hat{\Phi}_{j,l,k} = \hat{\Phi}_j(R_{\psi_l} \zeta) \exp(i \langle p_k^{j,l}, \zeta \rangle), \quad (2)$$

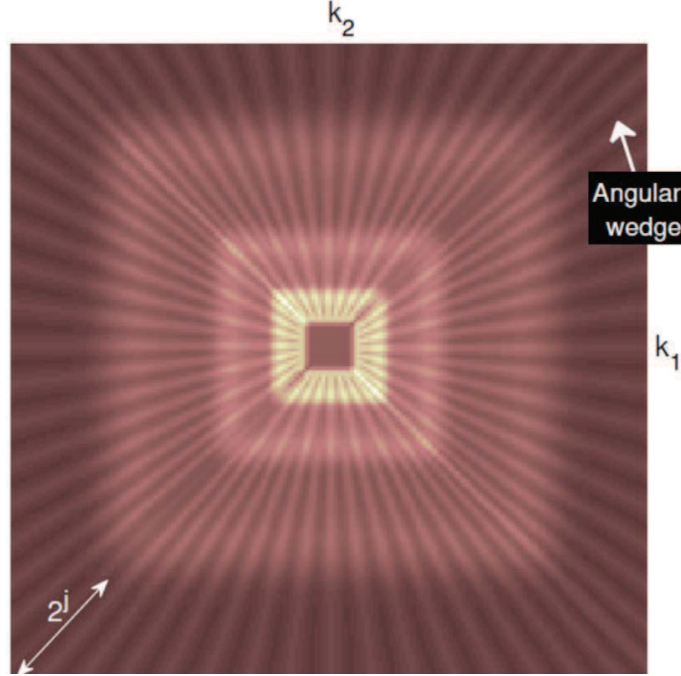


Figure 2: Default curvelet tiling.

where $p_k^{j,i} = R_{\psi_l}^{-1}(2^{-j}k_1, 2^{-j/2}k_2)$ and $\zeta = (\zeta_1, \zeta_2)$ are the cartesian coordinates in the frequency-domain. the rotation matrix R_{ψ_l} is given as:

$$R_{\psi_l} = \begin{pmatrix} \cos \psi_l & \sin \psi_l \\ -\sin \psi_l & \cos \psi_l \end{pmatrix}. \quad (3)$$

The curvelet transform of a function f is given by the convolutional integral:

$$c_{j,l,k} = \int f(x) \overline{\Phi_{j,l,k}(x)} = \langle f, \Phi_{j,l,k} \rangle dx. \quad (4)$$

The coefficients of the curvelet transform, $c_{j,l,k}$, in the above equation are interpreted as the decomposition of function f into the basis curvelet $\Phi_{j,l,k}$. The curvelet-domain frequency-domain view is shown in Fig. 2.

The filtering methodology works as follows. First, the image or 2D signal is transformed into the curvelet-domain, then thresholding is applied and finally, signal is reconstructed after noise removal. For removing the noise from the image using the curvelet transform, we apply the standard methodology [26,29,37,38] [25] which is outlined here for the sake of self-containedness and clarity. Let assume that the noisy data is represented as

$$x_{m,n} = I(m,n) + \sigma n_{m,n} \quad (5)$$

where I is the image of interest and n is the white noise with mean zero and variance 1, i.e. $n_{m,n} \sim N(0,1)$. Let F denotes the discrete curvelet transform matrix, then, we have $Fn \sim N(0, FF^T)$. Since the computation of the

transform domain variance FF^T is prohibitively expensive, therefore, it is calculated by an approximate value $\tilde{\sigma}_\lambda^2$ (where λ is the curvelet index) of the individual variances using Monte-Carlo simulations where the diagonal elements of FF^T are simply estimated by evaluating the curvelet transforms of a few standard white noise images. Let c_λ be the curvelet coefficients ($c = Fx$) corresponding to noise. The following hard-thresholding rule is used for removing noise

$$\hat{c}_\lambda = c_\lambda, \quad \text{if} \quad |c_\lambda|/\sigma \geq k\tilde{\sigma} \quad (6)$$

$$\hat{c}_\lambda = 0, \quad \text{if} \quad |c_\lambda|/\sigma < k\tilde{\sigma} \quad (7)$$

In our experiments, similar to [29], we actually chose a value for k which is scale-dependent; hence, we have $k = 4$ for the coarsest (first) scale ($j = 1$), whereas $k = 3$ for the other scales ($j > 1$).

4 Correlated Noise and Whitening Method

Curvelet transform based denoising performs most effectively under white noise scenario. The reason being that the threshold assumes white noise and that the noise samples are uncorrelated. For colored (correlated) noise, the performance is not as good as for uncorrelated noise (this is shown in the results section). In [25], the authors discussed the case of correlated noise, e.g., ground roll noise, however, they intuitively find the curvelet coefficients to be eliminated. To the best of our knowledge, this issue of threshold under the correlated noise case has not been addressed so far and previous works mainly used traditional methods.

Therefore, in this section, we introduce a simple yet effective technique to deal with this issue. We propose to use a whitening procedure to pre-whiten the data before curvelet-based processing in the case of colored noise. Here, we use the famous Zero-Phase Component Analysis (ZCA) for whitening. We start with Principal Component Analysis (PCA). Suppose, X is the image to be whiten. Note that, the columns of X are correlated, hence, in case of coherent correlated noise columns represent traces, whereas, in case of coherent noise rows represent traces. First, mean of each column is subtracted from the respective column. An estimate of the covariance matrix of the image X is then obtained as:

$$X^T X = U \Lambda U^T \quad (8)$$

where U is the square matrix whose i^{th} column is the eigenvector u_i of $X^T X$ and Λ is the diagonal matrix whose diagonal elements are the corresponding eigenvalues. The whitening matrix W_p then becomes

$$W_p = U \Lambda^{-1/2} \quad (9)$$

and the whitened image is:

$$X_w = X W_p = X U \Lambda^{-1/2} \quad (10)$$

This transformation first rotates the variables using the eigen matrix U of the covariance of X . This results in orthogonal components but with, in general, different variances. To achieve whitened data the rotated variables are then scaled by the square root of the eigenvalues $\Lambda^{1/2}$. PCA whitening is probably the most widely applied whitening procedure due to its simplicity and relation to PCA. It can be seen that the PCA and ZCA whitening transformations are related by a rotation matrix U , so ZCA whitening can be interpreted as a rotation followed by scaling followed by the rotation U back to the original coordinate system. Here note that the whitening by PCA is not unique. Any rotation (multiplying with a orthogonal rotation matrix) will leave it whitened. Hence, taking in particular U from the covariance matrix and multiplying with the whitening matrix W_p obtained from PCA, makes it unique. The new whitening matrix W_z thus created form basis for ZCA. Therefore, the ZCA-whitening is given as

$$X_w = XW_z = XU\Lambda^{-1/2}U^T \quad (11)$$

$\Lambda^{-1/2}$ is a diagonal matrix with $1/(\sqrt{\lambda_i})$ on the diagonal. This is regularized to $1/(\sqrt{\lambda_i} + \epsilon)$, where $\epsilon = 0.0001$. The procedure for the case of correlated noise is as follows:

- The image is whitened by multiplying it with the whitening matrix W_z .
- Noise is estimated from the data (this will be discussed in the experimental results section)
- Then, the whitened data is denoised using the curvelet transform.
- Finally, the whitened denoised data is restored by multiplying with the pseudo-inverse of the whitening matrix, i.e., $(W_z^H W_z)^{-1} W_z^H$.

5 Experimental results and Noise Estimation

In this section, we will perform some experiments to test the proposed curvelet transform method and present our noise estimation approach based on the pattern of seismic images.

In the first experiment, the curvelet denoising performance is compared for general purpose images and seismic images. In the second experiment, the method to estimate noise from the seismic images for incoherent noise (correlated or uncorrelated) is introduced. In the third experiment, performance of curvelet transform is tested for correlated noise case, while pre-whitening/whitening inverse steps are introduced in the fourth experiment in order to enhance the performance of curvelet based denoising under the correlated noise scenario. Finally, in the last experiment, worst case of ground roll noise is tackled using the whitening/whitening inverse filters and noise estimation from the image.

5.1 Performance of curvelet transform for general purpose images and seismic images

In the first experiment, we compare the curvelet transform denoising performance for general purpose images and seismic images. An image of seismic section is shown in Fig. 3. For seismic images, we have used the Netherlands

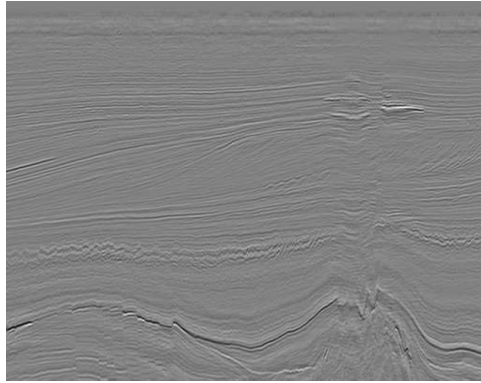


Figure 3: Samples of seismic images from the Netherlands offshore F3 block acquired in the North Sea with a resolution of $651 \times 951 \times 463$ (Crossline \times Inline \times Time).

offshore F3 block that is acquired in the North Sea having a resolution of $651 \times 951 \times 463$ (Crossline \times Inline \times Time). From this data set, twenty images are taken from inline # 30 to 600 with a gap of 30 inline sections. White noise is added to this data set. The comparison of the two types of images is depicted in Fig. 4, which reveals that the performance of curvelet transform based denoising is better for seismic images. The reason being that the seismic data are more localized in time, frequency, and phase domain and better match with the abilities of curvelet transform, i.e., taking into account the regularity and curvature nature of edges. The Peak-Signal-to-Noise Ratio (PSNR) is calculated as in [39]. For general-purpose images, the authors assume that noise variance is known.

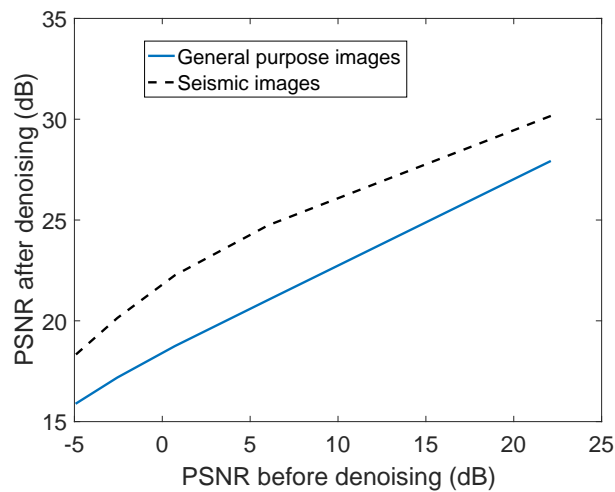


Figure 4: Performance of curvelet based denoising for general purpose images and seismic images.

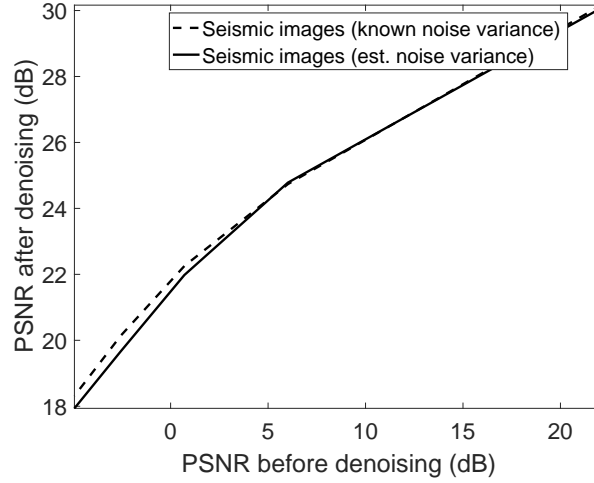


Figure 5: PSNR improvement for seismic images with known and estimated noise variance.

5.2 Noise variance estimation

The value of the noise variance is needed for thresholding in the curvelet domain [26]. Previous works (mentioned before) about the curvelet-based denoising rely on the a priori known value of the noise variance. However, in reality the variance is not known and hence, curvelet transform-based denoising need to be performed using hit and try method. This, in turn, adds to the complexity of already heavy computational load of the curvelet transform. In previous experiments, the variance was assumed to be known. Here, we estimate the variance using the image first 20×20 patch. Due to the pattern of the seismic image, the assumption here is that there is no signal of interest (seismic signal) in this patch, which is quiet true. The assumption fits in the case of noise that is not generated by the source signal. The comparison of the PSNR for known and estimated noise variance is shown in Fig. 5. The figure depicts that the curvelet based denoising achieves almost the same performance with known noise variance and the estimated one. These excellent results with noise variance estimation motivated us to use it for the rest of our experiments.

5.3 Correlated Noise

In the aforementioned experiments white noise is used and curvelet-based denoising gives promising results. It is important to check its performance in correlated noise, which is likely to be present in the seismic data, e.g. ground roll noise. For the correlated noise, we generated a noise with a $1/|f|^\alpha$ spectral characteristic over its entire frequency range. Most common values for α are $\alpha = 1$ (pink noise) and $\alpha = 2$ (brown or brownian noise). Brownian noise is considered to be the worst correlated noise in seismic applications. Note that $\alpha = 0$ refers to white noise. The autocorrelation and power spectrum density of various types of noises are shown in Fig. 6.

Comparison of the curvelet-based denoising under the correlated (color) and uncorrelated (white) noise reveals that the curvelet transform does not perform equally well in the later case (Fig.7). Hence, there is still room for the performance improvement. One reason of sub-optimal performance is that the noise samples are correlated and the other reason is

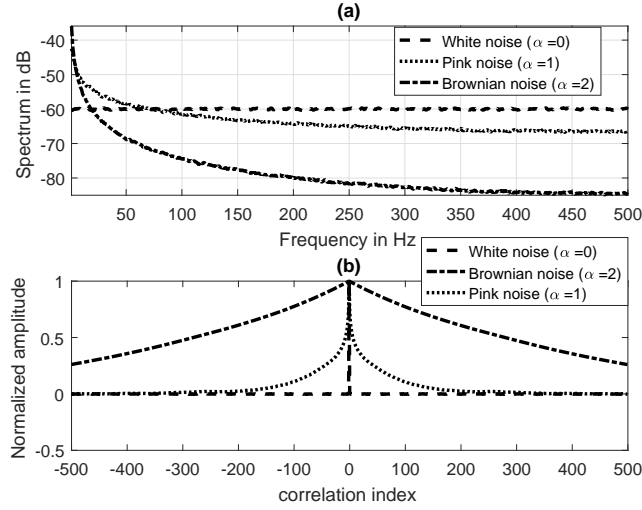


Figure 6: Noise specifications, (a) power spectral density, (b) autocorrelation function.

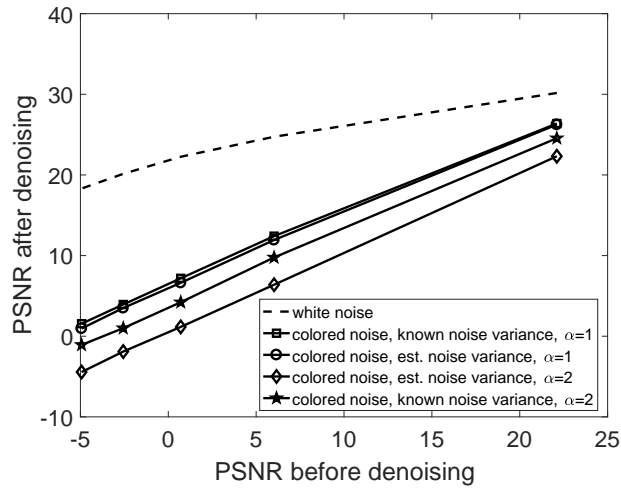


Figure 7: PSNR improvement for seismic images for various noises without whitening filter.

the threshold which assumes white noise. Furthermore, for the case of correlated noise the noise level in each curvelet is different and, hence, defining a global threshold does not give best performance. One complex and difficult way is to identify the curvelets that contain noise and define a curvelet dependent threshold based on the amount of noise in each curvelet. However, here we propose to include a pre-whitening filter the makes the noise to distribute equally among all the curvelets and apply the noise estimation method describe previously to get the similar performance as uncorrelated noise.

5.4 Whitening filter

To further improve the performance of curvelet-based denoising in correlated noise case, a pre-whitening filter (explained previously) is used. The pre-whitening filter makes the image uncorrelated and hence, application of curvelet

transform based denoising gives better results (close to white noise case). However, using pre-whitening on the noisy image some seismic signal information might be lost. For this purpose, after the denoising step using curvelet transform, whitening inverse filter is applied to get the final denoised image. The noise estimation is performed as before using first 20×20 patch from the pre-whitened seismic image. Figure 8 shows the autocorrelation matrix of the image before and after whitening using ZCA. It can be seen from the figure that the covariance matrix after denoising is diagonalized. The noisy and denoised (with and without whitening filter) is shown in Fig. 9. The performance difference of curvelet-based denoising with and without whitening can be clearly seen from the figure. From the Fig. 10, it can be seen that the $f - k$ magnitude spectra of the denoised seismic image closely matched with the $f - k$ spectra of noise-less seismic image. The PSNR plot for the various noise cases and whitening method is depicted in Fig. 11. The whitening method achieves close performance to that of the white noise case. The explicit PSNR values before and after denoising are shown in Table 1. Note here that the noise is estimated from the seismic image as before, which confirms that the noise estimation method gives best performance for incoherent noise case (either correlated or uncorrelated). In order to show the performance superiority of the proposed method, the technique is compared with the wavelet decomposition and empirical mode decomposition. For the wavelet decomposition based denoising technique, we use “wden” function in the wavelet toolbox of Matlab [40]. Moreover, we use the principle of Stein’s Unbiased Risk for soft thresholding (for details see wavelet toolbox in Matlab2017 and references [41] and [42]). The comparison is shown in Table 2.

5.5 Field data set with ground roll noise

To test the proposed method on field data with real noise (ground roll in this case), we used pre-stacked 2D land line from east Texas, USA. The ground roll noise have low apparent velocity, low frequency and high amplitude. For field data set, same procedure of denoising as before is used. First data is whitened using whitening filtering. Second, the curvelet-based denoising is used, i.e., data is transformed to the curvelet-domain and thresholding is used for noise attenuation. Third, denoised pre-whitened data obtained using inverse curvelet-transform. Finally, data is recovered using whitening inverse filter. Here, taking the first 20×20 patch for noise estimation is not a good choice as in this patch there is no coherent noise. The reason being that the noise is generated by the source (i.e., it is not a background noise like incoherent noise). For noise estimation in case of coherent noise, we proceed as follows: Considering the pattern of the ground roll noise seismic image, the patch at a furthest location directly under the shot location is assumed to be the signal only and the patch beside this is assumed to be contain the signal and noise. From these two patches the noise can be estimated using subtraction. After subtraction the variance (or standard deviation) of noise can be found for thresholding. The field data set, whitened data, denoised data and the difference between denoised and field data set is shown in Fig. 12. The patches are shown in the Fig. 12b by windows (signal-only part by black window, S and noise plus signal part by grey window, S_n). Using the windows, the variance is calculated as

$$\sigma^2 = E[(S_n(:) - S(:))^2] \quad (12)$$

Table 1: PSNR before and after denoising for various types of noises

PSNR before denoising (dB)	PSNR after denoising (dB)					
	without pre-whitening			with pre-whitening		
	$\alpha = 0$	$\alpha = 1$	$\alpha = 2$	$\alpha = 0$	$\alpha = 1$	$\alpha = 2$
-4.93	18.32	0.956	-4.93	18.32	18.00	17.64
-2.55	20.14	3.50	-1.90	20.14	20.05	19.24
0.71	22.26	6.62	1.15	22.26	22.15	20.81
6.02	24.74	11.93	6.38	24.74	24.58	23.76
22.11	30.16	26.24	22.32	30.16	28.01	28.01

where, $E[\cdot]$ represents the statistical expectation, and $S_n(\cdot)$ and $S(\cdot)$ represents the elements of the matrix S_n and S , respectively, arranged in a vector. Note that, in (12) the independence between the signal and the noise cannot be assumed, since noise is a function of the source signal.

In summary, whitening filter provides a threefold advantage.

- First, noise estimation is carried out easily from the seismic image for coherent and incoherent cases. This is a simple and straightforward method without much human intervention when compared to estimating the noise in the curvelets domain by identifying the curvelets corresponding to noise and excluding them for reconstructing of the seismic signal as done in [25].
- Second, the performance of curvelet based denoising is improved for correlated and coherent noise cases (after whitening noise become random) and get close to the best denoising performance under the random noise case. It is known that denoising methods performs better in random noise case.
- Third, the conventional hard thresholding method that assume white noise becomes valid.

6 Discussion and Conclusion

Typical seismic data exhibit low SNR and correlated noise. Removing noise will drastically improve signal detection, seismogram composition studies, and source discrimination for small local/regional seismic sources. In this work, we proposed a method based on the curvelet transform. The curvelet transform is a higher dimensional generalization of the wavelet transform, which is designed to represent images at different scales and different angles. It basically overcomes the problem of missing directional selectivity of the wavelet transforms in images. Comparison of the curvelet transform denoising performance for general purpose images and seismic images shows that is better for seismic images. The reason being that the seismic data are more localized in time, frequency and phase which better match the properties of curvelet transform. The noise variance needed for the threshold was estimated from the image patches themselves. For incoherent correlated (pink and brown noise) and coherent noise cases, a pre-whitening filter is introduced to enhanced the performance of curvelet denoising under colored noise. This makes the curvelet performs as good as in the case of white noise. Extensive testing of the proposed method on seismic images with incoherent (uncorrelated and correlated) and coherent noise shows very promising performance.

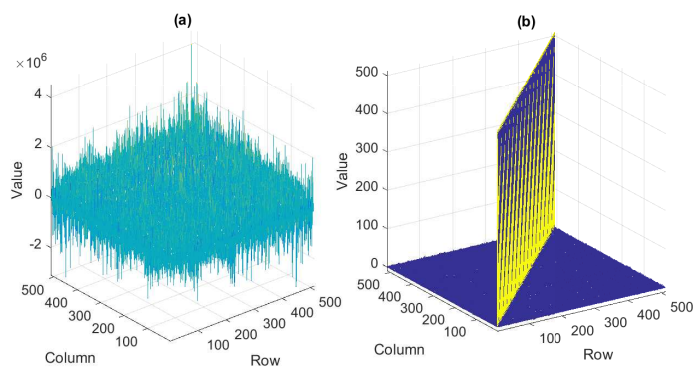


Figure 8: Covariance matrix of the noisy seismic image (a) before pre-whitening, (b) after pre-whitening.

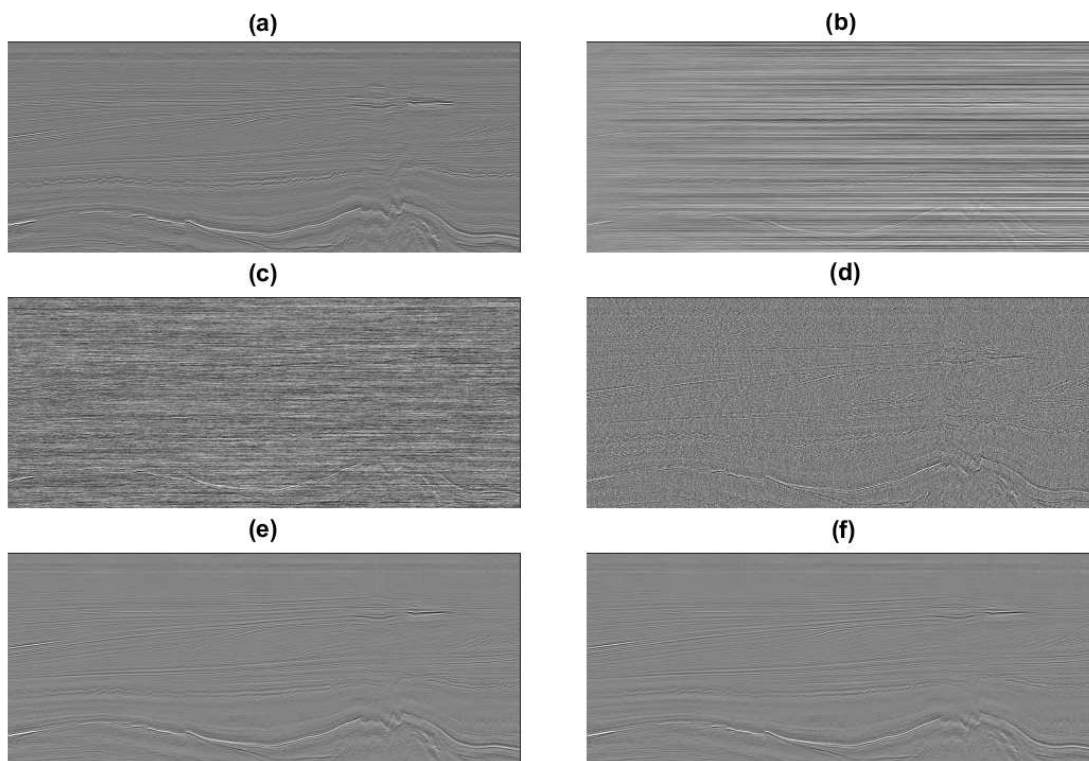


Figure 9: (a) Noise-less seismic image, (b) Noisy seismic image, $\alpha = 2$, PSNR before denoising = 5 dB. (c) Denoised image using curvelet without pre-whitening, (d) pre-whitened image, (e) denoised pre-whitened image together with whitening inverse ($\alpha = 2$), (f) denoised pre-whitened image together with whitening inverse ($\alpha = 1$).

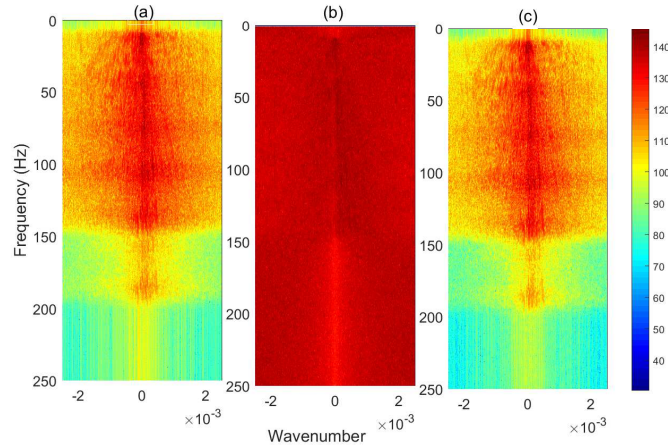


Figure 10: $f-k$ magnitude spectra: (a) Noise-less seismic data, (b) Noisy seismic data, $\alpha = 2$, PSNR before denoising = 5 dB. (c) Denoised seismic data.

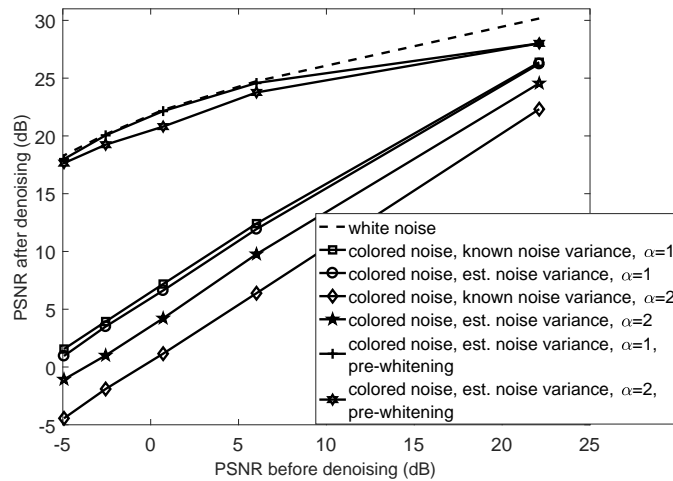


Figure 11: PSNR improvement for seismic images with various noises with pre-whitening.

References

- [1] T. Shirzad and Z.-H. Shomali, “Extracting seismic body and rayleigh waves from the ambient seismic noise using the rms-stacking method,” *Seismological Research Letters*, vol. 86, pp. 173–180, Jan. 2015.
- [2] J. Diaz, J. Gallart, and M. Ruiz, “On the ability of the benford’s law to detect earthquakes and discriminate seismic signals,” *Seismological Research Letters*, vol. 86, pp. 192–201, Jan. 2015.
- [3] I. F. Jones and I. Davison, “Seismic imaging in and around salt bodies,” *Interpretation*, vol. 2, pp. SL1–SL20, Nov. 2014.
- [4] T. J. Ulrych, M. D. Sacchi, and J. M. Graul, “Signal and noise separation: Art and science,” *GEOPHYSICS*, vol. 64, pp. 1648–1656, Sept. 1999.

Table 2: Comparison of the proposed method with other denoising methods.

Method	PSNR (dB)
Noisy data set	0.710
Wavelet decomposition	11.366
Empirical Mode Decomposition	10.524
Proposed method	22.26

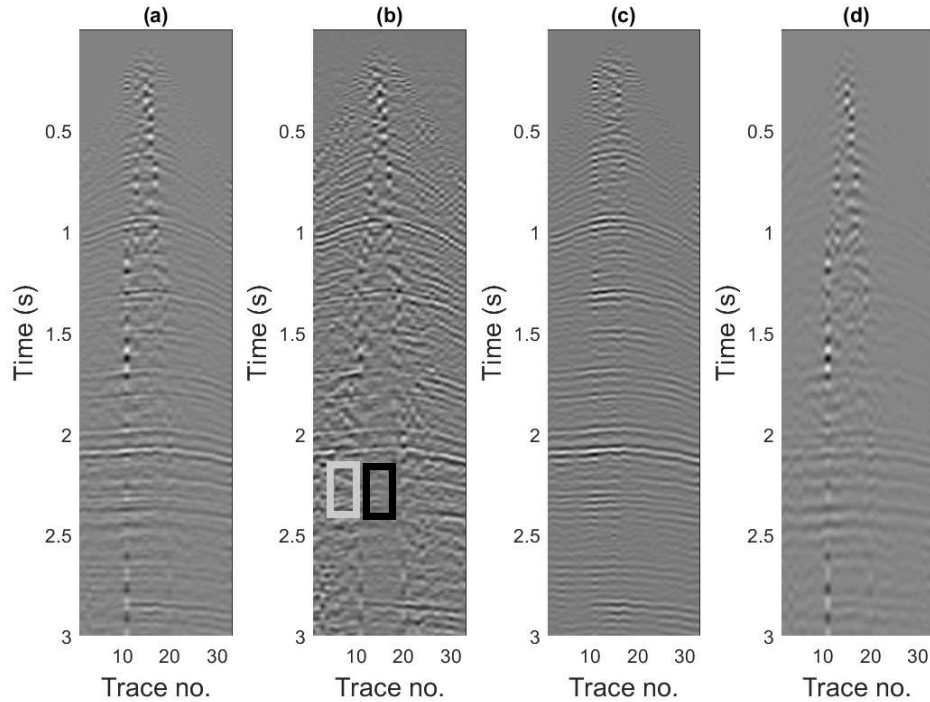


Figure 12: Seismic field data (shot gather number 8). (a) before denoising, (b) after whitening, (c) after denoising and applying whitening inverse, (d) difference image of (a) and (c).

- [5] H. Karsli and Y. Bayrak, "Ground-roll attenuation based on wiener filtering and benefits of time-frequency imaging," *The Leading Edge*, vol. 27, pp. 206–209, Feb. 2008.
- [6] A. Aghayan, P. Jaiswal, and H. R. Siahkoohi, "Seismic denoising using the redundant lifting scheme," *GEOPHYSICS*, vol. 81, pp. V249–V260, May 2016.
- [7] P. Bormann, *Seismic sources and source parameters*. New Manual of Seismological Observatory Practice (NMSOP-2), Potsdam, Germany: IASPEI, GFZ German Research Centre for Geosciences., 2012.
- [8] R. D. Peters, "Pink color of seismic noise in the low frequency limit," 2009.
- [9] M. S. Hons and R. R. Stewart, "Transfer functions of geophones and accelerometers and their effects on frequency content and wavelets," *CREWES Research Report*, vol. 18, 2006.
- [10] L. C. Duval and T. Røsten, "Filter bank decomposition of seismic data with application to compression and denoising," in *SEG Technical Program Expanded Abstracts 2000*, pp. 2055–2058, Society of Exploration Geophysicists, Jan. 2000.

- [11] S. A. F. Rastegar, A. Javaherian, N. K. Farajkhah, M. S. Monfared, and A. Zarei, "Effective parameters in ground roll attenuation using f0 crs stacking," *Journal of Applied Geophysics*, vol. 135, pp. 249–260, Dec. 2016.
- [12] A. Özbek, "Adaptive beamforming with generalized linear constraints," in *SEG Technical Program Expanded Abstracts 2000*, pp. 2081–2084, Society of Exploration Geophysicists, Jan. 2000.
- [13] P. Kearey, M. Brooks, and I. Hill, *An Introduction to Geophysical Exploration*. Blackwell Science, 2002.
- [14] J. Alcalde, C. E. Bond, G. Johnson, J. F. Ellis, and R. W. Butler, "Impact of seismic image quality on fault interpretation uncertainty," *GSA Today*, Feb. 2017.
- [15] K. J. Marfurt and T. M. Alves, "Pitfalls and limitations in seismic attribute interpretation of tectonic features," *Interpretation*, vol. 3, pp. SB5–SB15, Feb. 2015.
- [16] H. Jędrzejowska-Tyczkowska, "The influence of disturbances and noise of normal distribution on the correctness of geological interpretation of seismic sections with increased resolution," *Nafta-Gaz*, vol. 71, pp. 931–943, Dec. 2015.
- [17] E. Baziw, "Real-time seismic signal enhancement utilizing a hybrid rao-blackwellized particle filter and hidden markov model filter," *IEEE Geoscience and Remote Sensing Letters*, vol. 2, pp. 418–422, Oct. 2005.
- [18] X. Deng, H. Ma, Y. Li, and Q. Zeng, "Seismic random noise attenuation based on adaptive time-frequency peak filtering," *Journal of Applied Geophysics*, vol. 113, pp. 31–37, Feb. 2015.
- [19] E. Baziw and I. Weir-Jones, "Application of kalman filtering techniques for microseismic event detection," *Pure and Applied Geophysics*, vol. 159, pp. 449–471, Jan. 2002.
- [20] H.-P. Cai, Z.-H. He, and D.-J. Huang, "Seismic data denoising based on mixed time-frequency methods," *Applied Geophysics*, vol. 8, pp. 319–327, Dec. 2011.
- [21] S. P. Ghael, A. M. Sayeed, and R. G. Baraniuk, "Improved wavelet denoising via empirical wiener filtering," in *Proceedings of SPIE - The International Society for Optical Engineering* (A. Aldroubi, A. F. Laine, and M. A. Unser, eds.), pp. 389–399, Oct. 1997.
- [22] W. Lu, "Adaptive noise attenuation of seismic images based on singular value decomposition and texture direction detection," *Journal of Geophysics and Engineering*, vol. 3, pp. 28–34, Mar. 2006.
- [23] M. Coughlin, J. Harms, N. Christensen, V. Dergachev, R. DeSalvo, S. Kandhasamy, and V. Mandic, "Wiener filtering with a seismic underground array at the sanford underground research facility," *Classical and Quantum Gravity*, vol. 31, p. 215003, Nov. 2014.
- [24] W. A. Mousa and A. A. Al-Shuhail, "Processing of seismic reflection data using matlab™," *Synthesis Lectures on Signal Processing*, vol. 5, pp. 1–97, Sept. 2011.
- [25] M. Oliveira, M. Henriques, F. Leite, G. Corso, and L. Lucena, "Seismic denoising using curvelet analysis," *Physica A: Statistical Mechanics and its Applications*, vol. 391, pp. 2106–2110, Mar. 2012.

- [26] R. Neelamani, A. I. Baumstein, D. G. Gillard, M. T. Hadidi, and W. L. Soroka, "Coherent and random noise attenuation using the curvelet transform," *The Leading Edge*, vol. 27, pp. 240–248, Feb. 2008.
- [27] A. Górszczyk, A. Adamczyk, and M. Malinowski, "Application of curvelet denoising to 2d and 3d seismic data — practical considerations," *Journal of Applied Geophysics*, vol. 105, pp. 78–94, June 2014.
- [28] A. Górszczyk, M. Malinowski, and G. Bellefleur, "Enhancing 3d post-stack seismic data acquired in hardrock environment using 2d curvelet transform," *Geophysical Prospecting*, vol. 63, pp. 903–918, July 2015.
- [29] Jean-Luc Starck, E. Candes, and D. Donoho, "The curvelet transform for image denoising," *IEEE Transactions on Image Processing*, vol. 11, pp. 670–684, June 2002.
- [30] E. Candès, L. Demanet, D. Donoho, and L. Ying, "Fast discrete curvelet transforms," *Multiscale Modeling & Simulation*, vol. 5, pp. 861–899, Jan. 2006.
- [31] A. Kourav and P. Singh, "Review on curvelet transform and its applications," *Asian Journal of Electrical Sciences*, vol. 2, no. 1, pp. 9–13, 2013.
- [32] J. Ma and G. Plonka, "A review of curvelets and recent applications," *IEEE Signal Processing Magazine*, 2009.
- [33] E. J. Candès and D. L. Donoho, *Curvelets - A Surprisingly Effective Nonadaptive Representation For Objects with Edges*. Vanderbilt University Press, 2000.
- [34] Z. Long, Y. Alaudah, M. Quresh, M. Farraj, Z. Wang, A. Amin, M. Deriche, and G. AlRegib, "Characterization of migrated seismic volumes using texture attributes: a comparative study," in *Expanded Abstracts of the SEG 85th Annual Meeting, New Orleans, Louisiana*, pp. 1811–1815, 2018.
- [35] J. Li, R. Qi, Y. Zhang, and B. Xiong, "Higher-order correlative stacking for seismic data denoising based on the multiple-domain combination," *Near Surface Geophysics*, vol. 15, no. 3, pp. 260–273, 2017.
- [36] J.-H. Li, Y.-J. Zhang, R. Qi, and Q. H. Liu, "Wavelet-based higher order correlative stacking for seismic data denoising in the curvelet domain," *IEEE Journal of Selected Topics in Applied Earth Observations and Remote Sensing*, vol. 10, pp. 3810–3820, Aug. 2017.
- [37] T. Nguyen and Y. Liu, "Seismic noise attenuation using curvelet transform and dip map data structure," June 2017.
- [38] D. Shi and B. Milkereit, "Seismic signal enhancement using 2d fast discrete curvelet transform — an application to vsp and common-shot gathers from a hardrock environment," *GeoConvention*, 2015.
- [39] H. Al-Marzouqi and G. AlRegib, "Curvelet transform with learning-based tiling," *Signal Processing: Image Communication*, vol. 53, pp. 24–39, Apr. 2017.
- [40] M. Misiti, Y. Misiti, G. Oppenheim, and J. Poggi, "Wavelet toolbox for use with matlab," *The MathWorks, Natick, MA*, 1996.
- [41] S. M. Mousavi and C. A. Langston, "Hybrid seismic denoising using higher-order statistics and improved wavelet block thresholding," *Bulletin of the Seismological Society of America*, vol. 106, pp. 1380–1393, Aug. 2016.

- [42] C. Stein, "Estimation of the mean of a multivariate normal distribution," *Annals of Statistics*, vol. 9, no. 6, pp. 1135–1151, 1981.